Site and Isotopic Effects on the Angular Anisotropy of Products in the Photodissociation of Ethene at 157 nm

Shih-Huang Lee* and Yao-Chang Lee

National Synchrotron Radiation Research Center, 101 Hsin-Ann Road, Hsinchu Science Park, Hsinchu 30076, Taiwan

Yuan T. Lee

Institute of Atomic and Molecular Sciences, Academia Sinica, P.O. Box 23-166, Taipei 106, Taiwan

Received: August 8, 2005; In Final Form: November 24, 2005

We measured angular-anisotropy parameters $\beta(E_t)$ of fragments from photolysis of ethene and four isotopic variants at 157 nm using photofragment translational spectroscopy and selective photoionization. The averaged β value of products ranges from −0.17 to 0.10, depending on dissociation pathways. Angular distributions of atomic hydrogen produced from C_2H_4 and C_2D_4 are isotropic. For dissociation into $C_2H_2 + H_2$, β has a small negative value whereas dissociation into $C_2D_2 + D_2$ has an isotropic angular distribution. The photolysis of dideuterated ethene reveals site and isotopic effects on the angular distributions of products; products H_2, HD, and D_2 from photolysis of *1,1*-CH_2CD_2 have negative, nearly zero, and positive values of β, respectively. Molecular hydrogen from photolysis of *1,2-cis*-CHDCHD has a negative β value and the anisotropy has a trend $D_2 > H_2 > HD$. Photolysis of *1,2-trans*-CHDCDH produced a result similar to photolysis of *1,2-cis*-CHDCHD for the angular anisotropy of molecular hydrogen except slightly more isotropic. A calculation of optimized geometries of ethene in the ground electronic state and pertinent transition structures enables a qualitative interpretation of the site and isotopic effects on the angular anisotropy of products. We deduce that the photoexcited state of ethene at 157 nm has a major character $^1B_{1u}$ that produces a transition dipolar moment parallel to the C═C bond.

I. Introduction

Several experiments[1−5] have been devoted to absorption spectra of ethene in the vacuum ultraviolet (VUV) region. Figure 1 shows an absorption spectrum of ethene from 53 000 to 93 000 cm^{-1}; in the low energy part, the spectrum shows distinct intense features from 57 200 to 63 400 cm^{-1}, weak features from 63 400 to 70 800 cm^{-1}, and a broad underlying continuum from 53 000 to 70 800 cm^{-1}. Theoretical calculations[6−8] of electronic structure have been performed for electronic states of ethene, but the assignment of transitions pertinent to VUV absorption spectra is still controversial. We use the following assignments for electronic states. Five electronic states $\pi-\pi^*$ ($1\ ^1B_{1u}$), $\pi-3s$ ($1\ ^1B_{3u}$), $\pi-3p_y$ ($1\ ^1B_{1g}$), $\pi-3p_z$ ($1\ ^1B_{2g}$), and $\pi-3p_x$ ($2\ ^1A_g$) contribute to absorption below 68 000 cm^{-1}. Term symbols related to orbitals $3p_{x,y,z}$ are based on an orientation of ethene for which in the ground electronic state all atomic centers in their equilibrium positions lie within the $y-z$ plane with the C═C bond along the *z*-axis. The intense features from 57 200 to ∼63 400 cm^{-1} are attributed to the $\pi \rightarrow 3s$ transition, less intense features from ∼63 400 to ∼68 000 cm^{-1} are ascribed to transitions of the $\pi \rightarrow 3p$ manifold, and the broad underlying continuum is attributed to the $\pi \rightarrow \pi^*$ transition. One-photon transitions from the ground electronic state $1\ ^1A_g$ to states $1\ ^1B_{1g}$, $1\ ^1B_{2g}$, and $2\ ^1A_g$ have formally zero oscillator strength by virtue of a transition g → g being forbidden. According to a theoretical investigation,[8] the $1\ ^1B_{1g}$ surface intersects the $1\ ^1B_{1u}$ surface at a torsional angle of 24°; the $1\ ^1B_{1g}$ state can thereby borrow absorption intensity from the $1\ ^1B_{1u}$ state. The three components of the $\pi \rightarrow 3p$ transition were investigated through electron impact[9,10] and two-photon absorption spectra.[11,12] The absorption at wavenumbers greater than 68 000 cm^{-1} is attributed to transitions to higher Rydberg states.

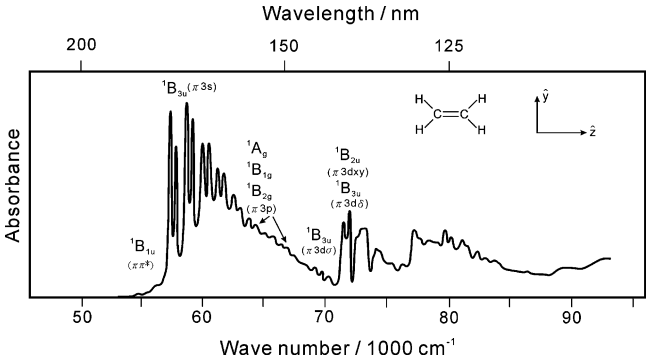

Figure 1. Absorption spectrum of ethene in the VUV region, adapted from ref 5.

As the smallest olefin and as an important species in atmospheric phenomena, ethene attracts interest in its photodissociation dynamics.[13−18] In the VUV region ethene has four dissociation pathways: $C_2H_3 + H$, $C_2H_2 + 2H$, $C_2H_2 + H_2$, and $H_2CC + H_2$. The C_2H_3 (vinyl) fragment with internal energy greater than ca. 36 kcal mol^{-1} dissociates further to $C_2H_2 + H$.[18] The elimination of H_2 from ethene involves three site-specific dissociation pathways via *1,1*, *1,2-cis*, and *1,2-trans* mechanisms.[19−21] The former process first produces H_2CC

* To whom correspondence should be addressed. E-mail: shlee@nsrrc.org.tw.

10.1021/jp054414w CCC: $33.50
Published on Web 02/01/2006

(vinylidene), followed by rapid isomerization to HCCH (ethyne) with a forward barrier of 1.38 kcal mol^{-1}.[21] In the latter two processes an H atom first migrates to the other carbon atom to form CH_3CH (ethylidene), followed by elimination of H_2 from the CH_3 moiety to produce ethyne. The branching ratios of the four product channels depend on excitation energy. Time-of-flight (TOF) spectra of photofragments from photolysis of ethene at 193 nm[13−15] and 157 nm[16−18] were investigated with the use of a molecular-beam apparatus. For photolysis at 193 nm, the distributions of kinetic energy for elimination of H and H_2 were measured, and the dependence of kinetic-energy release on the vibration−rotational state of H_2 was investigated.[15] Electron-impact ionization[16,17] and photoionization[18] were used to detect fragments from photolysis of ethene at 157 nm. Products H, H_2, C_2H_2, and C_2H_3 were successfully detected with synchrotron radiation whereas only H and H_2 were reported with electron-impact ionization. Branching ratios and distributions of kinetic energy of photofragments have been measured for photolysis of ethene in five isotopic variants.

The angular distribution of a photofragment pertains to the angle between recoil velocity v of the fragment and transition dipolar moment μ of its parent molecule. For randomly orientated molecules, their products that recoil parallel and perpendicular to μ have angular anisotropies (β) of 2 and −1, respectively, in the laboratory frame.[22] An understanding of angular distributions of products facilitates not only the recognition of fragmentation but also the assignment of the photoexcited state. Two electronic states, $1\ ^1B_{1g}$ ($\pi-3p_y$) at 7.80 eV[11,12] and $1\ ^1B_{2g}$ ($\pi-3p_z$) at 7.90 eV,[11] of ethene have energies near that of the present excitation energy of 7.87 eV (157.6 nm), but they have formally zero oscillator strength for a one-photon excitation as mentioned above. Our objectives in the present work are to determine the major photoexcited state of ethene at 157 nm from measurements of the angular anisotropy of products and to reveal site and isotopic effects on the angular distributions of products.

II. Experimental Section

The apparatus is described in detail elsewhere.[18,23] Briefly, our molecular-beam machine comprises two source chambers, a reaction chamber and a detection chamber. By means of several turbomolecular pumps backed with dry fore pumps, the pressure of the molecular-beam machine without gas loading attained less than 2×10^{-8} Torr. A liquid-nitrogen trap and a He refrigerator were employed in combination to suppress residual gas, especially H_2, to 5×10^{-12} Torr in the ionization region. A F_2 excimer laser provided radiation at 157 nm for photolysis, and the synchrotron in the National Synchrotron Radiation Research Center (NSRRC) provided VUV radiation to ionize photofragments. A solenoid valve (with orifice of diameter 0.5 mm) located in the source chamber served to expand samples into the reaction chamber with a backing pressure of 300 Torr. The samples were pure ethene (C_2H_4), *1,1-d*$_2$-ethene (*1,1*-CH_2CD_2), *1,2-cis-d*$_2$-ethene (*1,2-cis*-CHD-CHD), *1,2-trans-d*$_2$-ethene (*1,2-trans*-CHDCDH), and d_4-ethene (C_2D_4). We detected no fragmentation of ethene clusters under these conditions of expansion. The molecular beam was collimated with two successive skimmers. To prevent molecules from rebounding from an outlet surface into the detector, we installed a copper panel (with an orifice of diameter 3 mm) just beyond the outlet of the source chamber and chilled it to 18 K with a He refrigerator. The dissociating beam of radiation was introduced into the reaction chamber along the pivot of the rotating source assembly and intercepted the molecular beam perpendicularly. We selected dissociating light at a linear polarization with two thin-film polarizers (Laseroptik GmbH) arranged in a V shape. To avoid complication from multiphoton processes we set the photon flux to 50−100 μJ mm^{-2} $pulse^{-1}$. The dispersion of the velocities of photofragments occurred along a flight path of length 100 mm before these species became ionized. An undulator installed in the storage ring of NSRRC provided radiation, and the Chemical Dynamics beamline delivered it to the ionization region of the molecular-beam machine. Radiation from the undulator has a highly oscillatory distribution of photon energy due to interference; the maxima occur at fundamental, second harmonic, third harmonic, ... frequencies. Because only photons at the fundamental frequency were desired for the present experiments, we equipped this beamline with a windowless cell filled with noble gas to absorb photons at high harmonics. An optical filter of MgF_2 served to absorb residual photons at high harmonics effectively when the energy of the fundamental photons was less than 10 eV. After ionization, ions were extracted into a quadrupole mass filter to select a desired ratio m/z of mass to charge. A detector of Daly type counted ions and a multichannel scaler displayed ion signals on a computer versus flight time. Background spectra were recorded when not negligibly small. Subtraction of the background spectra and the flight interval of ions from the raw spectra yielded TOF spectra of products. All TOF spectra were recorded at 250 ns per channel. A pulse generator operating at 75 Hz synchronized components of the experimental apparatus.

III. Computations

Chang et al. have calculated the optimized structures of transition states and intermediates on the ground-state potential-energy surface of ethene at the B3LYP/6-311G(d,p) level.[21] Because the Cartesian coordinates of atoms are not reported in the literature, we recalculated the optimized geometry of ground-state ethene and its transition structures ts1, ts2, and ts4 for elimination of molecular hydrogen with a program GAUSSIAN 98 at a level of B3LYP/aug-cc-pVTZ. As previously defined,[21] ts1, ts2, and ts4 correspond to transition states on dissociation paths from CH_2CH_2 to intermediate $CHCH_3$, from $CHCH_3$ to $CHCH + H_2$, and from CH_2CH_2 to $CH_2C + H_2$, respectively. Vector displacements of atoms in transition structures ts2 and ts4 were computed for ethene in five isotopic species. The lengths of C═C and C−H bonds of ground-state ethene were computed to be 1.325 and 1.082 Å respectively; ∠CCH is 121.7°. For elimination of atomic hydrogen, an optimized structure with a carbon−hydrogen bond fixed at 2.082 Å was calculated for ethene in all isotopic species involving H and D.

IV. Results and Analysis

We measured TOF spectra of fragments upon photolysis of ethene in five isotopic forms using dissociating light with linear polarizations at α, α + 90°, α + 180°, and α + 270° relative to the detection axis. Angle α that corresponds to a maximum or minimum of signal in the laboratory frame depends on the recoil velocity of a fragment; for simplicity, angle α averaged over all velocities was adopted for each fragment in this paper. The averaged value of α is less than 5° for atomic and molecular hydrogen. To diminish systematic error we summed TOF spectra recorded at α and α + 180° to form a parallel (∥) spectrum and summed α + 90° and α + 270° spectra to form a perpendicular (⊥) spectrum. For brevity, only the most pertinent TOF spectra are presented here. Figure 2 shows ∥ and ⊥ TOF spectra of products at m/z 2−4 and 26−28 after photolysis of *1,1*-CH_2-CD_2. Partitions of product TOF spectra have been previously

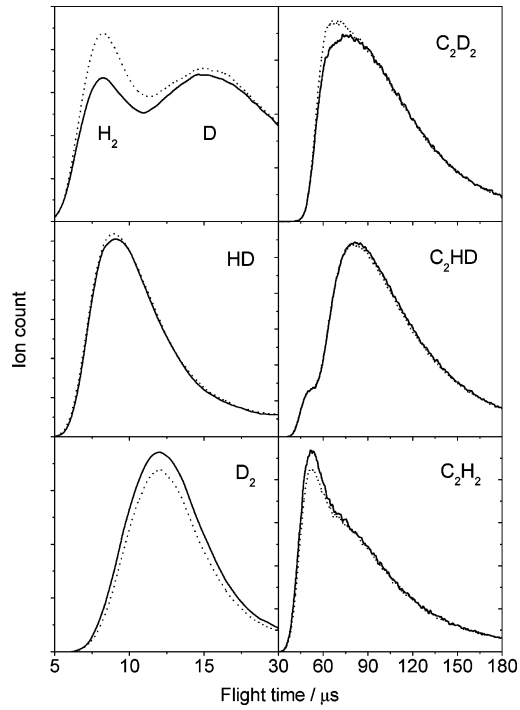

Figure 2. TOF spectra of products at *m*/*z* 2, 3, 4, 26, 27, and 28 after photolysis of *1,1*-CH_2CD_2. Products at *m*/*z* 2−4 (26−28) were detected at a laboratory angle of 30° (15°), using ionizing photons at 17.0 eV (12.8 eV). TOF spectra were recorded using dissociating light with polarization parallel (solid line) and perpendicular (dotted line) to the TOF axis.

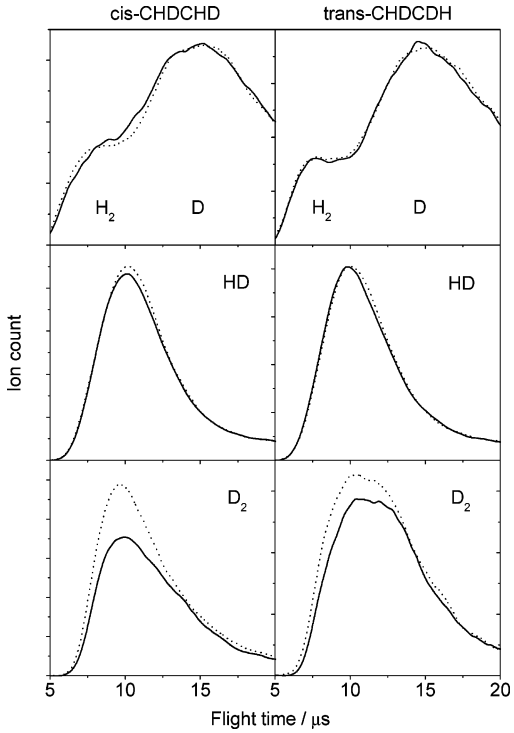

Figure 3. TOF spectra of products at *m*/*z* 2, 3, and 4 after photolysis of *1,2-cis*-CHDCHD and *1,2-trans*-CHDCDH. These products were detected at a laboratory angle of 30° using ionizing photons at 17.0 eV. TOF spectra were recorded with use of dissociating light with polarization parallel (solid line) and perpendicular (dotted line) to the TOF axis.

reported.[18] The rapid component of ethyne correlates with molecular hydrogen and the slow component is due to loss of two hydrogen atoms. Figure 2 indicates that two momentum-matched products, ethyne and molecular hydrogen, have the same behavior in the difference between || and ⊥ TOF spectra, which confirms the accuracy of the measured β values. Ethyne due to loss of two hydrogen atoms has an isotropic angular distribution, independent of isotopic variants of ethene. Figure 3 shows || and ⊥ TOF spectra of products at *m*/*z* 2, 3, and 4 from photolysis of *1,2-cis*-CHDCHD and *1,2-trans*-CHDCDH; these spectra were recorded using ionizing photons at 17.0 eV. The TOF spectra of atomic D were measured separately with ionizing photons at 14.0 eV, as shown in ref 18. TOF spectra of H_2 are thus obtained on subtracting the 14-eV spectra from the 17-eV spectra recorded at *m*/*z* 2 but not shown in this paper.

The angular distribution of a product with a specific kinetic energy is expressible as

$$I_{cm}(E_t,\theta) = \frac{1}{4\pi} P(E_t)[1 + \beta(E_t)P_2(\cos\theta)] \qquad (1)$$

in the center-of-mass (c.m.) frame. $P(E_t)$ is the distribution of c.m. kinetic energy of product, and $\beta(E_t)$ is the distribution of the angular-anisotropy parameter as a function of E_t. E_t is the c.m. kinetic energy of products including two momentum-matched fragments. $P_2(\cos\theta)$ equals $(3\cos^2\theta - 1)/2$; θ is the angle between the recoil direction of a product and the linear polarization of the dissociating radiation. Using a computer program PHOTRAN based on forward convolution, we derived the $I_{cm}(E_t,\|)$ and $I_{cm}(E_t,\perp)$ spectra from the || and ⊥ TOF spectra, respectively. $\beta(E_t) = 2[I_{cm}(E_t,\|) - I_{cm}(E_t,\perp)]/[I_{cm}(E_t,\|) + 2I_{cm}(E_t,\perp)]$ is derivable from eq 1. Figure 4 summarizes $\beta(E_t)$ for elimination of molecular hydrogen from three dideuterated species of ethene. After photolysis of *1,1*-CH_2CD_2, the angular anisotropy of products from dissociation into $C_2D_2 + H_2$, C_2HD + HD, and $C_2H_2 + D_2$ has negative, nearly zero, and positive β values, respectively, which differs from the results of photolysis of *1,2-cis*-CHDCHD and *1,2-trans*-CHDCDH. The latter two have similar angular distribution of products; the elimination of molecular hydrogen has a negative β value and the anisotropy has a trend $D_2 > H_2 > HD$. The elimination of H_2 from C_2H_4 has a negative β value whereas the elimination

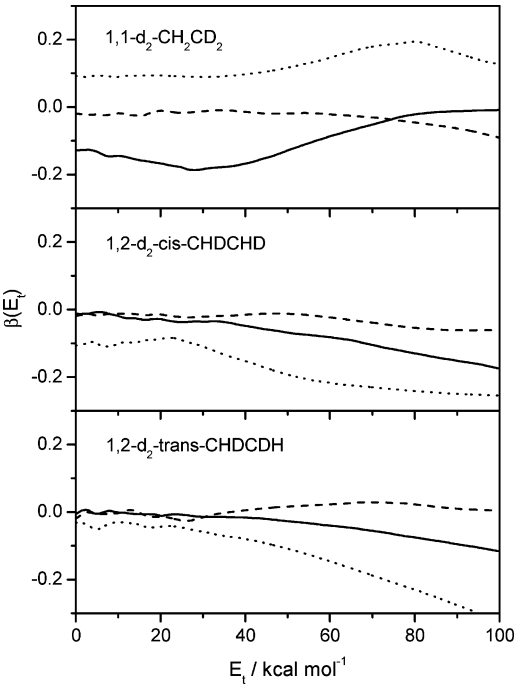

Figure 4. $\beta(E_t)$ for dissociation of $C_2D_2 + H_2$ (solid line), C_2HD + HD (dashed line), and $C_2H_2 + D_2$ (dotted line) from ethene in three dideuterated variants.

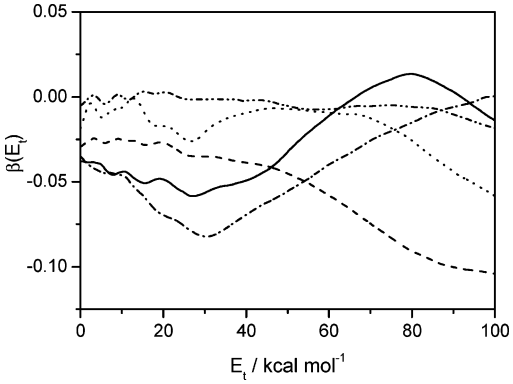

Figure 5. $\beta(E_t)$ of all molecular hydrogen, i.e., a sum of H_2, HD, and D_2, produced on photolysis of *1,1*-CH_2CD_2 (solid line), *1,2-cis*-CHDCHD (dashed line), *1,2-trans*-CHDCDH (dotted line), C_2H_4 (dash-dotted line), and C_2D_4 (dash-dot-dotted line).

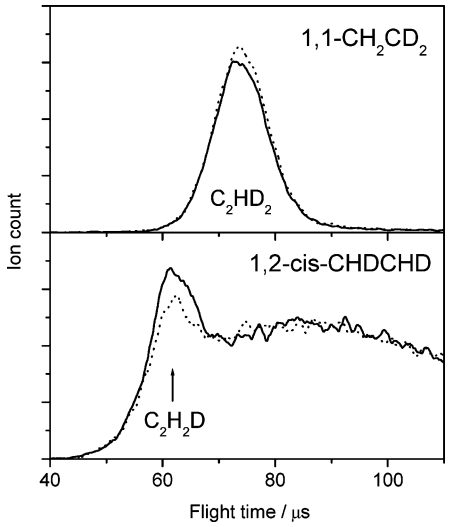

Figure 6. TOF spectra of products at *m/z* 29 and 28 after photolysis of *1,1*-CH_2CD_2 and 1,2-*cis*-CHDCHD, respectively. Products were detected at a laboratory angle of 15° using ionizing photons at 10.3 eV. The TOF spectra were recorded with use of dissociating light with polarization parallel (solid line) and perpendicular (dotted line) to the TOF axis.

of D_2 from C_2D_4 is isotropic. Figure 5 summarizes $\beta(E_t)$ averaged over all H_2, HD, and D_2 for ethene in five isotopic species; we employed product branching ratios 0.38:0.41:0.21, 0.16:0.71:0.13, and 0.16:0.71:0.13 for H_2:HD:D_2 of *1,1-d*$_2$-, *1,2-d*$_2$*-cis*-, and *1,2-d*$_2$*-trans*-ethene,[18] respectively, to yield the averaged $\beta(E_t)$. The angular distributions of atomic hydrogen are isotropic except for the C_2HD_2 + H dissociation from *1,1*-CH_2CD_2 and the C_2H_2D + D dissociation from *1,2-cis*-CHDCHD, as shown in Figure 6. Table 1 summarizes angular-anisotropy parameters $\langle\beta\rangle$ averaged over all kinetic energies with $P(E_t)$ as a weighting factor; the uncertainty of $\langle\beta\rangle$ is estimated to be 0.01. In the molecular frame the β parameter of a product pertains to the recoil angle γ of a product with respect to the transition dipolar moment μ of a parent molecule and is expressible as $\langle\beta\rangle \cong 3\cos^2\langle\gamma\rangle - 1$; we thus derive $\langle\gamma\rangle$ from $\langle\beta\rangle$ as shown in Table 1. Three γ angles 0°, 54.7° (called the magic angle), and 90° lead to $\beta = 2$, 0, and -1, respectively.

We also calculated the γ value of a hydrogen molecule leaving ethene in an optimized transition structure to compare with the experimental $\langle\gamma\rangle$ value. Because structures of ethene were computed in a molecular frame, we aligned those structures of ethene from the ground state to a transition state in the laboratory frame, i.e., involving their relative orientations. For simplicity, we neglect the process of optical excitation to a higher electronic state followed by internal conversion back to the ground electronic state. This assumption is not completely unreasonable because the complicated vibrational motion of ethene prior to dissociation might not be a determinant on product angular anisotropy; the key point is the structure of ethene along a dissociating coordinate. We initially arranged ground-state ethene in the $y-z$ plane with the C=C bond along the *z*-axis, and then aligned the transition structures with respect to that of ground-state ethene according to conservations of center of masses and of angular momentum, i.e., $\vec{P} = \sum_i m_i \cdot \vec{v}_i = 0$ and $\vec{L} = \sum_i m_i(\vec{r}_i \times \vec{v}_i) = 0$. $\vec{P}$ and $\vec{L}$ are linear and angular momenta of ethene and are initially set to zero; *m*, *r*, and *v* denote atomic mass, coordinate, and velocity, respectively, and *i* denotes the index of an atom. Because the trajectories of atoms from ground-state ethene to a transition structure are unknown in the present work, we assumed that each atom has linear motion from the ground state to a transition state and thus $\sum_i m_i \cdot \Delta\vec{r}_i/\Delta t = 0$ and $\sum_i m_i(\vec{r}_i \times \Delta\vec{r}_i)\Delta t = 0$; $\Delta\vec{r}$ denotes an atomic displacement from the ground state to a transition structure after a duration of Δt. In the present calculation, we assumed that transition state ts4 is a gateway for 1,1-elimination (1,1-E) of molecular hydrogen, and transition states ts1 and ts2 are two sequential gateways for 1,2-elimination (1,2-E) of molecular hydrogen. Figure 7 shows the structures of the ground state and transition states ts2 and ts4 of ethene for elimination of H_2, HD, and D_2 from *1,1*-CH_2CD_2. Structure ts1[21] serves as the first step in determining the orientation of ts2 but is not shown here. To facilitate comparison, the leaving hydrogen molecule is arranged at the bottom of ethene. *1,1*-CH_2CD_2 undergoes a 1,1-E process for elimination of H_2 and D_2, and a 1,2-E process for HD elimination. The latter process involves two mechanisms: migration of an H atom to form $CHCHD_2$ followed by HD elimination (i.e., 1,2-E on the D side), and migration of a D atom to form $CDCH_2D$ followed by HD elimination (i.e., 1,2-E on the H side). Figures 8 and 9 show the structures of ethene in its ground state and the transition state for elimination of H_2, HD, and D_2 from *1,2-cis*-CHDCHD and *1,2-trans*-CHDCDH, respectively. State ts4 for 1,1-elimination of HD from *1,2-cis*-CHDCHD and *1,2-trans*-CHDCDH has two structures with HD wagging to the H side (i.e., 1,1-E on the H side) and to the D side (i.e., 1,1-E on the D side). Elimination of 1,2-HD from *1,2-cis*-CHDCHD involves migration of a D atom to form $CHCHD_2$ followed by HD elimination (i.e., 1,2-E on the H side), and migration of an H atom to form $CDCH_2D$ followed by HD elimination (i.e., 1,2-E on the D side). Elimination of H_2 and D_2 from *1,2-trans*-CHDCDH implies a 1,2-E mechanism. Elimination of H_2 (D_2) from *1,2-cis*-CHDCHD requires, however, cis → trans isomerization or a torsional motion of intermediate $CDCH_2D$ ($CHCHD_2$) if ts2 is a gateway for H_2 (D_2) elimination; we refrain here from tackling this complicated problem. The various recoil angles of molecular hydrogen were evaluated from the computed vector displacements of molecular hydrogen with respect to the *z*-axis and are listed in Table 1.

Because elimination of atomic hydrogen has no transition state, the recoil direction of atomic hydrogen is estimated from the difference between ethene in an optimized structure that has a carbon−hydrogen bond fixed at 2.082 Å and the equilibrium structure of ground-state ethene. The recoil angles of atomic hydrogen were calculated with respect to the *z*-axis (i.e., the initial axis of the C=C bond) and are listed in Table 1.

TABLE 1: Averaged β Values and Corresponding Recoil Angles γ of Products after Photolysis of Ethene in Three Dideuterated Species At 157 nm[a]

	1,1-CH_2CD_2		*1,2-cis*-CHDCHD		*1,2-trans*-CHDCDH	
product channel	$\langle\beta\rangle$	$\langle\gamma\rangle$/deg	$\langle\beta\rangle$	$\langle\gamma\rangle$/deg	$\langle\beta\rangle$	$\langle\gamma\rangle$/deg
$C_2HD_2 + H$	−0.04	56 (59)	∼0	55 (58)	∼0	55 (58)
$C_2H_2D + D$	∼0	55 (55)	0.08	53 (56)	∼0	55 (56)
$C_2D_2 + H_2$	−0.16	58 (67)	−0.06	56	−0.02	55 (59)
$C_2HD + HD$	−0.02	55 (56;[b] 68[c])	−0.02	55 (57;[b] 59;[d] 64;[e] 68[c])	∼0	55 (59;[d] 63[e])
$C_2H_2 + D_2$	0.10	53 (56)	−0.17	58	−0.10	57 (62)

[a] Numbers in parentheses are theoretical results. [b] 1,2-E on the D side. [c] 1,2-E on the H side. [d] 1,1-E on the H side. [e] 1,1-E on the D side.

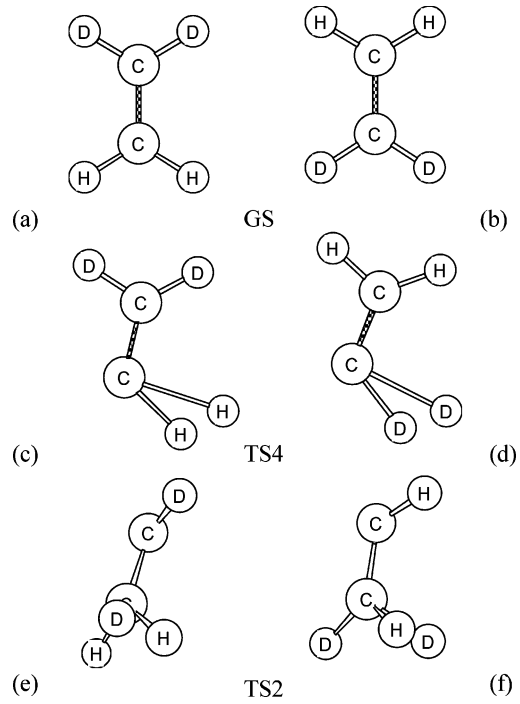

Figure 7. Transition structures ts4 and ts2 for elimination of molecular hydrogen from *1,1*-CH_2CD_2. Ground-state ethene, GS (a and b), lies with atomic centers in the $y-z$ plane with the C═C bond along the *z*-axis. Structures c and d depict the transition states ts4 for elimination of H_2 and D_2, respectively. Structures e and f depict the transition states ts2 for elimination of HD via migration of a D- and H-atom, respectively. Recoil angles of molecular hydrogen from structures c, d, e, and f are calculated to be 67°, 56°, 68°, and 56°, respectively, with respect to the *z*-axis.

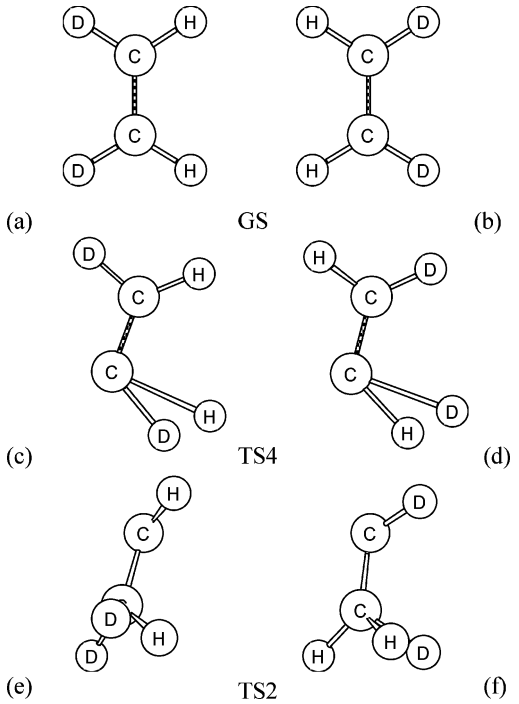

Figure 8. Transition structures ts4 and ts2 for elimination of molecular hydrogen from 1,2-*cis*-CHDCHD. Ground-state ethene, GS (a and b), lies with atomic centers in the $y-z$ plane with the C═C bond along the *z*-axis. Structures c and d depict transition states ts4 for elimination of HD on the H side and on the D side, respectively. Structures e and f depict transition states ts2 for elimination of HD via migration of a D- and H-atom, respectively. The recoil angles of molecular hydrogen from structures c, d, e, and f are calculated to be 59°, 64°, 68°, and 57°, respectively, with respect to the *z*-axis.

V. Discussion

A transition state plays a particularly crucial role in a dissociation that just surmounts the energy of that state. Rice−Ramsperger−Kassel−Marcus (RRKM) theory employs the nature of a transition state to evaluate a rate coefficient for dissociation and further branching ratios.[20,21] Several theoretical models, such as an impulsive model or transition-state theory and its variants, also employ a transition structure to evaluate energy disposal and the population of products in quantum states. Moreover, the angular distribution of a product might also pertain to a transition structure if the transition state is a gateway for dissociation. Although a dissociating molecule might not exactly surmount the saddle point of a transition structure, that structure provides more or less information on angular distributions of products. Products from separate chemical sites have distinct recoil directions and thus varied angular distributions. Deuterium is typically used to label dissociation from a specific chemical site, but deuterium substitution in ethene might alter the center of total mass, the vector displacements of atoms during molecular deformation, and the molecular orientation in the laboratory frame. We previously[18] reported site and isotopic effects on branching ratios and distributions of kinetic energy; these two effects on product angular anisotropy are revealed in this paper. We interpreted the angular distributions of products according to the following scheme. First, internal conversion of ethene from the photoexcited state to the ground electronic state is extremely rapid. Second, following internal conversion, ethene dissociates through a transition structure that is rotated with respect to the initial orientation of ethene. Third, the angular anisotropy of a product is determined by the angle γ between the recoil direction of a product and the transition dipolar moment of ethene. Fourth, a large vibrational energy might cause ethene to dissociate through a structure far from the minimum in a transition state, and parent rotation might decrease the angular anisotropy of products.

A. Elimination of Molecular Hydrogen. C_2H_4 and C_2D_4 have a small angular anisotropy with $\langle\beta\rangle = -0.06$ and ∼0, respectively, in elimination of molecular hydrogen, which is attributed mainly to averaging over all chemical sites. Site and isotopic effects on the angular anisotropy of products are observed in the photolysis of ethene in three dideuterated species. We surmised that H_2 and D_2 produced on photolysis

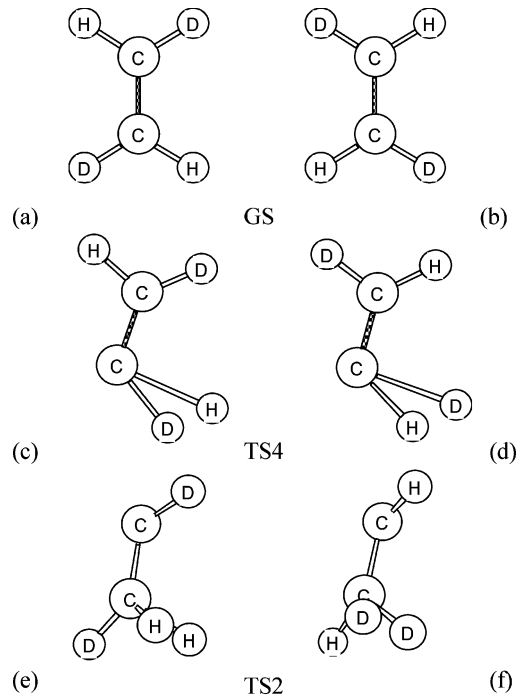

Figure 9. Transition structures ts4 and ts2 for elimination of molecular hydrogen from 1,2-*trans*-CHDCDH. Ground-state ethene, GS (a and b), lies with its atomic centers in the *y*−*z* plane with the C═C bond along the *z*-axis. Structures c and d depict transition states ts4 for elimination of HD on the H side and on the D side, respectively. Structures e and f depict transition states ts2 for elimination of H_2 and D_2 via migration of an H- and D-atom, respectively. The recoil angles of molecular hydrogen from structures c, d, e, and f are calculated to be 59°, 63°, 59°, and 62°, respectively, with respect to the *z*-axis.

of *1,1*-CH_2CD_2 have the same angular anisotropy before performing this experiment because they occupy chemically identical sites of ethene, but eliminations of H_2 and D_2 from a dideuterated species have disparate β values, even though they come from chemically identical sites. The present theoretical calculations for the direction of product recoil enable a qualitative interpretation of our observations about the angular anisotropy of products. Because atomic H is less massive than atomic D, according to conservation of angular momentum structure ts4 of *1,1*-CH_2CD_2 has an angle γ for H_2 larger than that for D_2 in the laboratory frame; see Figure 7. An analogous argument is applicable to the photolysis of *1,2-trans*-CHDCDH for which H_2 has a smaller recoil angle than D_2; see Figure 9. The elimination of H_2 and D_2 from *1,2-cis*-CHDCHD requires cis → trans isomerization to form *1,2-trans*-CHDCDH or a torsional motion along the C−C bond of the ethylidene intermediate for state ts2 to be the gateway for elimination of H_2 and D_2.

Elimination of HD from *1,1*-CH_2CD_2, *1,2-cis*-CHDCHD, and *1,2-trans*-CHDCDH has nearly isotropic angular distributions, which we attribute mainly to an average of at least two dissociation mechanisms; see Figures 7−9. Our present theoretical calculation indicates that elimination of HD from *1,1*-CH_2CD_2 has two mechanisms via migration of an D and H atom, to form transition structure ts2 of $CDCH_2D$ and $CHCHD_2$, respectively, followed by HD elimination. As D is twice as massive as H, $CDCH_2D$ has a γ value larger than $CHCHD_2$ for HD elimination. The elimination of HD from *1,2-trans*-CHDCDH involves two ts4 structures with HD wagging to the H and D sides, respectively; the former structure has a γ value smaller than the latter because of the mass effect. *1,2-cis*-CHDCHD has four mechanisms to eliminate HD; two dissociations proceed via ts2 states and two others proceed via ts4 states. Table 1 indicates that the theoretical values of $\langle\gamma\rangle$ are somewhat larger than the experimental values, although their trends are in agreement. The discrepancy is partly due to uncertainty in the present theoretical calculation and partly due to the large excitation energy, 181.4 kcal mol^{-1}. After internal conversion, a large vibrational energy (e.g., 74 kcal mol^{-1} in ts2 and 88 kcal mol^{-1} in ts4) increases the probability of dissociation trajectories occurring far from the saddle point (vide infra). Thus, elimination of H_2 and D_2 from *1,1*-CH_2CD_2 occurs at γ angles less than 67° and 56°, respectively.

Figure 4 indicates that $\beta(E_t)$ for elimination of H_2 and D_2 from a dideuterated ethene appears to have similar distributions but a shift in magnitude. The same mechanism to eliminate H_2 and D_2 from a dideuterated ethene accounts for the similarity in their β distributions with E_t; the aforementioned mass effect is responsible for the shift in the magnitude of β. Based on $\beta \cong 3\cos^2\gamma - 1$, a variation of β with kinetic energy might be regarded as a variation of γ with kinetic energy. Using a trajectory model to simulate the angular distributions of products from a triatomic dissociating system, Loock et al.[24] found that the angular anisotropy of a product depends significantly on the bending motion of the triatomic molecule if the transition dipolar moment lies in the molecular plane, whereas the dependence becomes weak if the transition dipolar moment is perpendicular to the molecular plane. As in the present work the transition dipolar moment of ethene is parallel to the C═C bond (vide infra), and molecular hydrogen can alter its recoil angle γ through the bending motion of the C−C−H_2. Ethene with a greater bending motion of C−C−H_2 spreads molecular hydrogen into a wider angle (i.e, becoming more isotropic) and causes fragments to become more rotationally excited (i.e., having less kinetic energy). The variation of angular anisotropy of a product with kinetic energy pertains to dissociation dynamics and warrants further theoretical investigation. Moreover, Figure 5 indicates that an isotopic effect remains even though hydrogen molecules from all chemical sites are included.

B. Elimination of Atomic Hydrogen. Ethene has four chemically identical hydrogen atoms. For elimination of atomic H from *1,1*-CH_2CD_2 $\beta = -0.04$, whereas for elimination of atomic D from *1,2-cis*-CHDCHD $\beta = 0.08$; other processes to eliminate hydrogen from ethene in five isotopic species are isotropic. Because no transition state participates in elimination of atomic hydrogen, the recoil direction of a hydrogen atom might be evaluated from the structure of ethene in its ground state, for which the equilibrium −CCH angle is 121.7°.[21] If a hydrogen atom leaves along the direction of the carbon−hydrogen bond, the recoil direction of the hydrogen atom is ∼58.3° with respect to the C═C bond, which accounts for the intrinsically small angular anisotropy for atomic hydrogen. To express β as an isotopic dependence, we evaluated the recoil direction of atomic hydrogen from the displacement of a leaving hydrogen atom from its equilibrium position in ground-state ethene to a structure with a carbon−hydrogen bond fixed at 2.082 Å. During bond rupture the total angular momentum and center of masses of ethene are conserved. Our theoretical result indicates that elimination of atomic H from a dideuterated species of ethene has a γ value, 58−59°, larger than that for elimination of atomic D, $\gamma = 55-56°$, which is satisfactorily consistent with the experimental result. The present theoretical calculation is more applicable to elimination of atomic hydrogen than to elimination of molecular hydrogen. An elimination of atomic hydrogen after cis−trans isomerization is not taken into account in the present work.

In a consecutive ternary dissociation ABC → A + BC → A + B + C, the secondary fragments B and C commonly have a smaller angular anisotropy than the primary fragments A and BC by a factor of approximately $\langle P_2(\cos\delta)\rangle$; δ is an angle of the recoil direction of fragment B or C relative to the original flight direction of fragment AB. Because fragment AB is rotationally excited, the primary fragment spreads its secondary fragments into δ angles over a wide range, which thus decreases the resultant angular anisotropy of secondary fragments. A primary fragment with a lifetime much greater than its rotational period typically produces an isotropic angular distribution for secondary fragments. In the title reaction, after elimination of two hydrogen atoms ethyne has an isotropic angular distribution because the factor $\langle P_2(\cos\delta)\rangle$ is nearly zero.[18]

C. Photoexcited State. From the measured angular-anisotropy parameters of various fragments, we deduce that the transition dipolar moment of ethene at 157 nm might be parallel with the C═C bond of ethene in its electronic ground state. As mentioned in section I, only 1 $^1B_{1u}$ and 1 $^1B_{3u}$ states have nonzero oscillator strength in the absorption systems from 53 000 to 68 000 cm^{-1}; the transition 1 $^1A_g \rightarrow 1\ ^1B_{1u}$ produces a dipolar moment along the C═C bond and the transition 1 $^1A_g \rightarrow 1\ ^1B_{3u}$ produces a dipolar moment perpendicular to the molecular plane. Accordingly, we suggest that the photoexcited state of ethene at 157 nm has a major character of $^1B_{1u}$; ethene is excited either to a high vibrational level of state 1 $^1B_{1u}$ ($\pi-\pi^*$) or to state 1 $^1B_{1g}$ ($\pi-3p_y$) in which the latter transition borrows oscillator strength from the former.[8] With the same experimental apparatus, state 2 $^1A'$ ($\pi-3p$) has been identified as the major photoexcited state of propene at 157 nm.[23] The methyl substituent alters the symmetry from D_{2h} (ethene) to C_s (propene) and produces a nonzero oscillator strength for the three components of the $\pi \rightarrow 3p$ transition of propene.

Quantum-chemical calculations[25−27] indicate that a nonadiabatic transition (i.e., conical intersection) among three low-lying singlet states (i.e., N, V, and Z states according to Mulliken's notation) of ethene occurs through twisting the olefinic bond. To study the photoinduced cis−trans isomerization and nonadiabatic transition of ethene, Ben-Nun and Martinez[26] calculated the molecular dynamics in several electronic states. After photoexcitation ethene first stretches its C═C bond; a torsional motion along the C═C bond follows, and then a methylene group becomes pyramidal. The cis−trans isomerization of ethene begins at ∼50 fs in the excited electronic state through the torsional motion, and the first nonadiabatic event of ethene occurs at ∼250 fs through the motion into the pyramidal geometry after photoexcitation.[26] The rapid cis−trans isomerization is responsible for the similarity between *1,2-cis*-CHDCHD and *1,2-trans*-CHDCDH in kinetic-energy distributions and branching ratios of products.[18] For the angular anisotropy of the products, photolysis of *1,2-trans*-CHDCDH produces a result still similar to photolysis of *1,2-cis*-CHDCHD, but slightly more isotropic.

D. Vibrational and Rotational Effects. After ultrarapid internal conversion, the excitation energy 181.4 kcal mol^{-1} converts into vibrational energy of ethene in the electronic ground state. If the dissociation of ethene is extremely rapid, most energy is deposited into several vibrational degrees of freedom, and ethene dissociates through a route away from the energy minimum of a transition structure. If energy flow is more rapid than decomposition, a stationary vibrational motion normal to the dissociation coordinate of ethene in a transition structure has a smaller average effect on the angular anisotropy of a product. Comparison of product branching ratios between experiment[18] and RRKM calculation[21] indicates that the fragmentation of ethene after excitation at 157 nm is not fully statistical.

The rotational effect pertains to the lifetime of parent molecules. By means of a RRKM approach, Chang et al.[21] calculated rate coefficients for dissociation of ethene with internal energy equivalent to a photon of wavelength 157 nm; the rate coefficients for dissociation of C_2D_4 to C_2D_3 + D and $D_2CC + D_2$ are 3.74×10^{11} and 4.77×10^{11} s^{-1}, respectively. Moreover, C_2D_4 dissociates to CDCD + D_2 through an intermediate $CDCD_3$; the rate coefficients for $C_2D_4 \rightarrow CDCD_3$ and $CDCD_3 \rightarrow CDCD + D_2$ are 7.59×10^{11} and 2.31×10^{12} s^{-1}, respectively. From these RRKM calculations we estimate that the lifetime of internally hot ethene might be less than 1 ps. Rotational parameters *A* (4.828 cm^{-1}), *B* (1.0012 cm^{-1}), and *C* (0.8282 cm^{-1}) of C_2H_4 correspond to classical rotational periods 3.5, 16.6, and 20.1 ps along principal axes *a*, *b*, and *c*, respectively; a larger rotational quantum number produces a smaller rotational period. Rotation along the *a*-axis has no significant influence on the angular anisotropy of a product because the *a*-axis is parallel to the C═C bond and μ of ethene. Rotation along axes *b* and *c* of ethene before dissociation might alter the orientation of ethene and thus decrease the angular anisotropy of a product. In our experiment involving supersonic expansion in a molecular beam, ethene is cooled to several low rotational levels; our results indicate that rotation of ethene before fragmentation does not completely scramble the angular distributions of products.

Using classical mechanics for a symmetric top molecule, Yang and Bersohn[28] treated the effect of parent rotation on the angular anisotropy of products; this treatment averages over all rotational states of parent molecules according to a Boltzmann distribution and includes all allowed rotational transitions, i.e., in P, Q, and R branches. If the transition dipolar moment is along the top axis of a symmetric top molecule, the angular anisotropy of a product decreases with increasing lifetime and approaches $^1/_4$ or $^1/_6$ as the lifetime tends to infinity, but the rotation of a parent molecule does not alter the sign of β. This classical model is unsuitable to treat the angular distributions of products from parent molecules in a single rotational state. Using a quantum-mechanical model to treat the angular anisotropy of products with respect to parent rotation in a dissociating system with a long lifetime, Butenhoff et al.[29] found that the angular anisotropy β of H_2 ($v = 1$, $J = 0$) produced from photolysis of H_2CO varies in the range 0.05−0.54 with rotational quantum number $J \leq 4$ of H_2CO. Because ethene is a nearly prolate rotor, has μ parallel to the rotor axis, and dissociates rapidly after optical excitation, the model of Yang and Bersohn seems more suitable for interpretation of the rotational effect in our experiments than that of Butenhoff et al.

Overall, a large vibrational energy might cause fragmentation of ethene at angle γ away from a transition structure, and rotation of ethene before fragmentation might somewhat diminish the angular anisotropies of products. With rotation and vibration of parent molecules, it is, however, difficult to account for the isotopic effect on the angular anisotropy of products, particularly for the different sign of β of H_2 and D_2 produced from *1,1*-CH_2CD_2. The aforementioned mass effect plays a crucial role in differentiating the angular anisotropy of isotopic products.

VI. Conclusion

We investigated the angular anisotropies of photofragments upon photolysis of ethene and some isotopic variants thereof at

157 nm using a molecular-beam apparatus and synchrotron radiation. Photofragments from C_2H_4 and C_2D_4 have isotropic angular distributions except dissociation into $C_2H_2 + H_2$ that has $\beta = -0.06$. Elimination of atomic hydrogen from dideuterated species of ethene has an isotropic angular distribution except elimination of atomic H from *1,1*-CH_2CD_2 and atomic D from *1,2-cis*-CHDCHD. Product ethyne and its isotopic variants due to elimination of two hydrogen atoms have an isotropic angular distribution, reflecting a sequential ternary dissociation. Site and isotopic effects play significant roles in the angular distributions of molecular hydrogen. After photolysis of *1,1*-CH_2CD_2, H_2 has a negative β value whereas D_2 has a positive β value, although these two fragments come from two chemically identical sites; as HD arises from two dissociation pathways it has an isotropic angular distribution. The angular distributions of products from *1,2-cis*-CHDCHD are nearer those from *1,2-trans*-CHDCDH than those from *1,1*-CH_2CD_2; the former two have negative β values for molecular hydrogen as product and the angular anisotropy exhibits a trend $D_2 > H_2 >$ HD. In the title reaction, the proximity of the direction of product recoil to the magic angle leads to a small angular anisotropy with the value of $\langle\beta\rangle$ ranging from -0.17 to 0.10. Although the present theoretical calculation is rough, it indicates the key point for the dependence of the angular anisotropy of products on chemical sites and isotopic substitution. A further theoretical investigation with a trajectory model is worthwhile to improve the agreement in β values and to explore the dynamics of dissociation. In the photolysis of ethene, the isotopic (mass) effect is more significant in the angular distributions of products than in the distributions of kinetic energy. From our measurements of the angular anisotropy of products, we deduce that the photoexcited state of ethene has a major character of $^1B_{1u}$ at 157 nm, which produces a transition dipolar moment along the C═C bond of ethene in its electronic ground state. This transition might involve direct excitation to state 1 $^1B_{1u}$ ($\pi-\pi^*$) or excitation to state 1 $^1B_{1g}$ ($\pi-3p_y$) with intensity borrowed from the former transition. The effects of vibration and rotation of a parent molecule on the angular anisotropy of products are also addressed.

Acknowledgment. National Synchrotron Radiation Research Center, Academia Sinica, and the National Science Council of Taiwan (grant NSC94-2113-M-213-004) provided support for this work.

References and Notes

(1) Wilkinson, P. G.; Mulliken, R. S. *J. Chem. Phys.* **1955**, 23, 1895.

(2) Robin, M. B. *Higher Electronic States of Polyatomic Molecules*; Academic: New York, 1985; Vol. 3, pp 213−227 and references therein.

(3) Foo, P. D.; Innes, K. K. *J. Chem. Phys.* **1974**, 60, 4582.

(4) McDiarmid, R. *J. Phys. Chem.* **1980**, *84*, 64.

(5) Sension, R. J.; Hudson, B. S. *J. Chem. Phys.* **1989**, 90, 1377.

(6) (a) Rico, R. J.; Lee, T. J.; Head-Gordon, M. *Chem. Phys. Lett.* **1994**, 218, 139. (b) Head-Gordon, M.; Rico, R. J.; Oumi, M.; Lee, T. J. *Chem. Phys. Lett.* **1994**, 219, 21.

(7) Mebel, A. M.; Chen, Y.-T.; Lin, S.-H. *J. Chem. Phys.* **1996**, *105*, 9007 and references therein.

(8) Ryu, J.-S.; Hudson, B. S. *Chem. Phys. Lett.* **1995**, 245, 448.

(9) Ross, K. J.; Lassettre, E. N. *J. Chem. Phys.* **1966**, 44, 4633.

(10) Johnson, K. E.; Johnston, D. B.; Lipsky, S. *J. Chem. Phys.* **1979**, 70, 3844.

(11) Williams, B. A.; Cool, T. A. *J. Chem. Phys.* **1991**, 94, 6358.

(12) Gedanken, A.; Kuebler, N. A.; Robin, M. B. *J. Chem. Phys.* **1982**, 76, 46.

(13) Satyapal, S.; Johnston, G. W.; Bersohn, R. *J. Chem. Phys.* **1990**, 93, 6398.

(14) Balko, B. A.; Zhang, J.; Lee, Y. T. *J. Chem. Phys.* **1992**, *97*, 935.

(15) Cromwell, E. F.; A. Stolow, A.; Vrakking, M. J. J.; Lee, Y. T. *J. Chem. Phys.* **1992**, 97, 4029.

(16) Lin, J. J.; Hwang, D. W.; Lee, Y. T.; Yang, X. *J. Chem. Phys.* **1998**, 109, 2979.

(17) Lin, J. J.; Wang, C. C.; Lee, Y. T.; Yang, X. *J. Chem. Phys.* **2000**, 113, 9668.

(18) Lee, S.-H.; Lee, Y. T.; Yang, X. *J. Chem. Phys.* **2004**, 120, 10983.

(19) Jensen, J. H.; Morokuma, K.; Gordon, M. S. *J. Chem. Phys.* **1994**, 100, 1981.

(20) Chang, A. H. H.; Mebel, A. M.; Yang, X.-M.; Lin, S. H.; Lee, Y. T. *Chem. Phys. Lett.* **1998**, 287, 301.

(21) Chang, A. H. H.; Mebel, A. M.; Yang, X.-M.; Lin, S. H.; Lee, Y. T. *J. Chem. Phys.* **1998**, 109, 2748.

(22) Zare, R. N. Ph.D. Thesis, Harvard University, Cambridge, MA, 1964.

(23) Lee, S.-H.; Lee, Y. T. *Chem. Phys. Lett.* **2004**, 395, 311.

(24) Loock, H.-P.; Cao, J.; Qian, C. X. W. *Chem. Phys. Lett.* **1993**, 206, 422.

(25) Persico, M.; Bonacic-koutecky, V. *J. Chem. Phys.* **1982**, 76, 6018.

(26) Ben-Nun, M.; Martinez, T. J. *Chem. Phys. Lett.* **1998**, 298, 57.

(27) Ohmine, I. *J. Chem. Phys.* **1985**, 83, 2348.

(28) Yang, S.-C.; Bersohn, R. *J. Chem. Phys.* **1974**, 61, 4400.

(29) Butenhoff, T. J.; Carleton, K. L.; van Zee, R. D.; Moore, C. B. *J. Chem. Phys.* **1991**, 94, 1947.